Co-published by
Institute of Fluid-Flow Machinery
Polish Academy of Sciences
Committee on Thermodynamics and Combustion
Polish Academy of Sciences

http://www.imp.gda.pl/archives-of-thermodynamics/

Experimental Investigation of the Performance and Emission Characteristics of Cotton Seed Biodiesel / Diesel Blends with Titanium Dioxide Nanoparticles

Santhosh Kumar Dubba[a,b], Raminaidu Pisini[a], Durgaprasad Kelli[a*], Roopsandeep Bammidi[a], Jaya Prasad Vanam[c], Narayana Turali[a]

[a]Aditya Institute of Technology and Management, Tekkali 532201, Andhrapradesh, India
[b]Indian Institute of Technology, Roorkee 247667, Uttarakhand, India
[c]Jawaharlal Nehru Technological University, Kakinada 533003, Andhrapradesh, India
*Corresponding author email: durgaprasadnita@gmail.com

Received: 08.04.2025; revised: 01.07.2025; accepted: 10.07.2025

Abstract

This study uniquely investigates cotton seed oil as a biodiesel source, a less-explored feedstock, and evaluates the role of TiO_2 nanoparticles in enhancing performance and emission characteristics. The use of a variable compression ratio engine under diverse load conditions further distinguishes this work from existing studies on nanoparticle-blended biofuels. The biodiesel was produced via transesterification and blended at various proportions, with and without TiO_2 additives. Experimental tests were conducted on a variable compression ratio diesel engine under varying load conditions: one-fourth, half, three-fourths, and full load. The results were compared against conventional diesel fuel. Among the tested blends, B40 (40% biodiesel, 60% diesel) without TiO_2 exhibited the highest brake thermal efficiency, exceeding that of diesel by 5.4%, and achieved the highest mechanical efficiency (58.31%) at full load condition. Fuel consumption increased proportionally with load across all fuel types. Notably, B40 without TiO_2 also recorded the lowest hydrocarbon emissions, with a reduction of 34 ppm at full load, which corresponds to a 45% decrease compared to conventional diesel. Carbon monoxide emissions were effectively eliminated in TiO_2-blended fuels due to improved combustion. Additionally, nitrogen oxides emissions were reduced by 1.1% in B40 when TiO_2 was incorporated. Overall, the findings highlight that cotton seed biodiesel, particularly when enhanced with TiO2 nanoparticles, can offer substantial improvements in engine performance and emission control compared to conventional diesel.

Keywords: Biodiesel; Cotton seed biodiesel; Titanium dioxide; Transesterification; VCR engine; Nanoparticles

Vol. 46(2025), No. 3, 151–161; doi: 10.24425/ather.2025.156587

Cite this manuscript as: Dubba, S.K., Pisini, R., Kelli, D., Bammidi, R., Vanam, J.P., & Turali, N. (2025). Experimental Investigation of the Performance and Emission Characteristics of Cotton Seed Biodiesel / Diesel Blends with Titanium Dioxide Nanoparticles. *Archives of Thermodynamics*, 46(3), 151−161.

1. Introduction

Researchers dedicate their time and efforts to discover alternative fuels to replace petrochemical fuels [1–4]. Certainly, the researchers across the world also work in various fields to meet the environmental sustainability goals [5–10]. It is crucial, however, to develop alternative fuels with properties comparable to petroleum-based fuels. Biodiesel has emerged as a promising substitute, attracting significant attention due to its environmentally friendly characteristics. Coating diesel engine pistons with a combination of titanium aluminide and yttria-stabilised zirconia significantly improved brake thermal efficiency and reduced emissions when using gulmohar biodiesel blends, with optimal results observed at a 200 μm coating thickness [11]. The addi-

Nomenclature

M – mass, kg
t – time, s
T – temperature, °C

Greek symbols

ν – kinematic viscosity, cSt
ρ – density, g/cm^3

Subscripts and Superscripts

m – mean

Abbreviations and Acronyms

BTE – brake thermal efficiency
CO – carbon monoxide
CV – calorific value, kJ/kg
FC – fuel consumption, kg/h
HC – hydrocarbon
ME – mechanical efficiency
NaOH– sodium hydroxide
NO_x – nitrogen oxide
TiO_2 – titanium dioxide
VCR – variable compression ratio

tion of titanium oxide (TiO_2) nanoparticles to Chlorella vulgaris biodiesel blends significantly enhanced engine performance, reduced emissions (Carbon monoxide (CO), Hydrocarbon (HC), smoke), and improved tribological properties, with optimal results observed at 100 ppm concentration [12].

The study demonstrated that blending water hyacinth biodiesel with n-pentanol and diesel (WHB20D75P5) enhances engine performance and reduces HC and CO emissions, indicating its potential as a viable diesel alternative [13]. The cotton seed oil stands out as a viable option among potential biodiesel sources. Alabi et al. [14] examined the combustion properties of diesel-vegetable oil blends using an industrial fuel burner, providing insight into critical parameters influencing the feasibility of these alternative fuels in industrial applications. The effects of viscosity on vegetable oil-based fuels can be efficiently minimized by mixing with diesel. This drop in viscosity improves fuel atomization, increases combustion efficiency, and reduces nozzle obstructions. They observed that greater vegetable oil concentration reduces flame duration and stability, which is mostly due to the higher density and viscosity of vegetable oil. The effective use of Mimusops elangi methyl ester (MEME) blended with TiO_2 nanoparticles as a biodiesel alternative, highlighting improved engine performance and reduced emissions at an optimized injection pressure of 220 bar [15].

Jain et al. [16] investigated the potential of Nahar biodiesel blended with TiO_2 nanoparticles (NBD-TNP) as a sustainable diesel alternative, demonstrating improved performance, combustion efficiency, and reduced emissions at an optimized injection pressure of 260 bar. Musthafa et al. [17] conducted an experimental study to minimize NO_x emissions from palm oil methyl ester mixed with diesel fuel (B20) utilizing a cetane number improver – di-tert-butyl peroxide (DTBP), and to improve the ignition performance of the test fuel. B20 with additives improves thermal efficiency by 2−3.5% and reduces specific energy consumption by 10−15% when compared to diesel and B20 fuels. In exchange for a little rise in HC, the B20 gasoline without additives showed a significant reduction in CO and nitrogen oxide (NO_x). Machine learning models, particularly random forest regression, have been effectively applied to predict combustion characteristics such as cylinder pressure and heat release rate in dual-fuel diesel engines using sustainable fuel blends, demonstrating high predictive accuracy and potential for emission reduction [18].

Radhakrishnan Lawrence et al. [19] evaluated the performance and emission magnitude of a single cylinder compression ignition (CI) engine fuelled with M. Elangi methyl ester (MEME) blends including TiO_2 nano-additions. MEME20 + 25TiO_2 and MEME20 + 25TiO_2 @20%EGR fuels had higher brake thermal efficiency (3.6% and 2.8%, respectively) than MEME20 fuel at full load. The addition of TiO_2 nanoparticles to MEME20 gasoline reduced HC and CO emissions, but the EGR approach increased both emissions when compared to MEME20 fuel. Their findings further suggest that the MEME20 + 25TiO_2 @20%EGR with 35% urea injection with Titanium dioxide (TiO2) coated catalyst (SCR) technology improves engine performance and reduces exhaust emissions.

Keskin et al. [20] investigated the effect of biodiesel-diesel fuel blends, including acetylferrocene and palladium-based additives, on diesel engine performance and emissions. They also confirmed that CO and PM emissions were decreased by up to 60.07% and 51.33%, respectively. Jiaqiang et al. [21] evaluated the combined use of water additives and metal-based additives in biodiesel-diesel mix fuels. They conducted comparative studies on various combinations of biodiesel-diesel (B5), water (2%, 4%, and 6% wt.) and cerium oxide (CeO_2) nanoparticles (90 ppm) with pure diesel in terms of combustion emissions and performance. They have proven that the correct amount of water addition improves performance while decreasing CO, PM, NO_x, and HC emissions. Mehregan and Moghiman [22] evaluated the effects of nano-additives on the performance and emission characteristics of a mixed biodiesel. Their testing results revealed an increase in brake specific fuel consumption and brake thermal efficiency for manganese oxide and cobalt oxide nanoparticles mixed gasoline, while NO_x and CO emissions were significantly reduced. Soudagar et al. [23] conducted a comprehensive evaluation of the influence of nano-additives in diesel-biodiesel fuel blends on engine performance and emission parameters. They confirmed that the majority of the outcomes improved thermophysical parameters, increased heat transfer rate, and stabilized fuel blends. Furthermore, scientists discovered that the amount of nanofluid additives increased engine performance characteristics while decreasing exhaust emissions.

Figure 1 represents a comprehensive flow diagram illustrating the life cycle and energy cycle of biodiesel production and its investigation process. The primary source is, i.e. cotton crop cultivation, where cotton seeds are collected as a by-product for the purpose of biodiesel preparation. These seeds undergo an oil extraction process to produce raw oil. The extracted oil is subjected to transesterification, a chemical process that removes fatty acids and glycerine, converting the oil into biodiesel. To

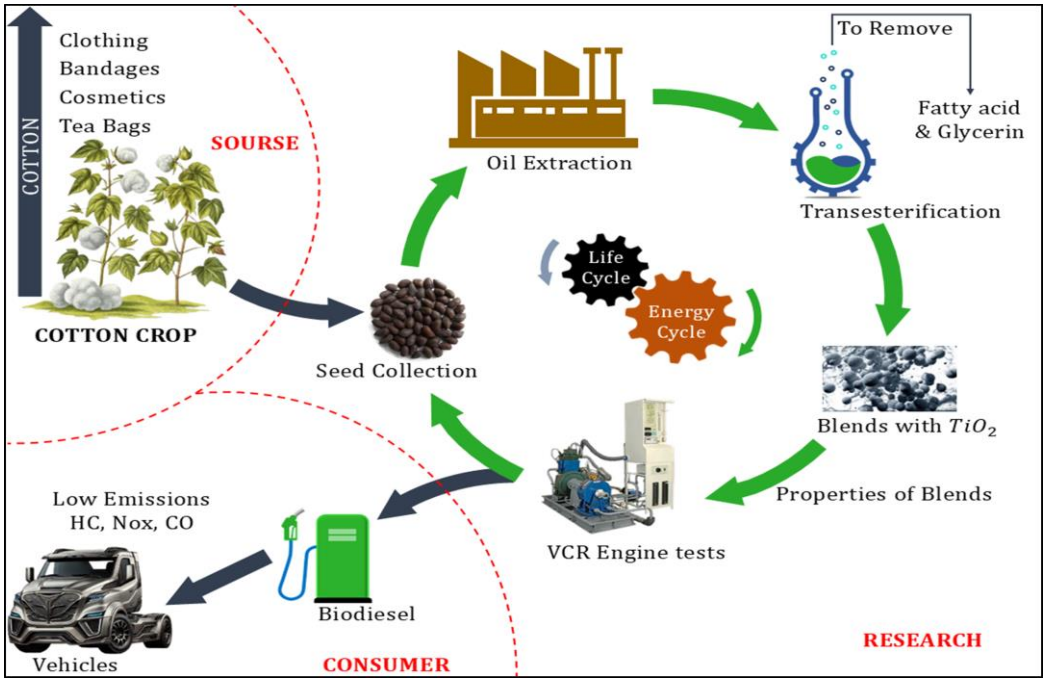

Fig. 1. Flow diagram illustrating the preparation and experimentation with blends – life cycle & energy flow cycle.

Fig. 2. Flow diagram of blends preparation.

enhance fuel properties, the biodiesel is blended with TiO_2 nanoparticles, forming experimental blends. Figure 2 also highlights the subsequent steps of evaluating the properties of these blends and testing their performance using a VCR engine.

The process contributes to the energy cycle by assessing emissions such as HC, NO_x and CO when used in vehicles, demonstrating low-emission outcomes. Additionally, the life cycle aspect integrates the biodiesel production process into practical applications, emphasizing sustainability and its potential to serve as an alternative fuel source. The overall figure connects source, research, and consumer applications, presenting a holistic approach to biodiesel production, experimentation, and utilization. This study investigates the performance and emission characteristics of cotton seed biodiesel-diesel emulsion blends with the addition of TiO_2 nanoparticles. The results are compared to those obtained using conventional diesel fuel. Cotton seed biodiesel was produced and tested under various loading conditions, utilizing a factorial design of experiments. The article examines the impact of different blends of this environmentally friendly alternative fuel on diesel engine performance and emission parameters.

2. Methodology

2.1. Preparation of biodiesel

The biodiesel was produced using cotton seeds obtained from local cotton farmers. Initially, the collected cotton seeds were sent to an oil extraction mill. The extracted oil was then subjected to a series of steps to produce biodiesel. A 1000 ml flat-bottom flask was selected as the reactor, which was placed on a magnetic stirrer set to maintain a temperature between 55°C and 60°C. The stirrer was positioned centrally to ensure uniform mixing of the reaction mixture. Before transesterification, the cotton seed oil underwent pre-treatment. The oil was first filtered to remove any solid impurities and then preheated to 100°C. It was maintained at this temperature for 25 minutes to eliminate moisture content, ensuring the oil was suitable for the biodiesel production process.

Subsequently, transesterification was carried out using a base-catalysed reaction to remove fatty acids and glycerine from the oil. A mixture of alcohol and catalyst was combined with 1000 ml of preheated cotton seed oil in the reactor, maintaining a temperature of 60−70°C. In a separate beaker, 4 grams of NaOH were dissolved (calculated as 3.8 grams per litre of oil: 3.5 grams stoichiometric equivalent plus 0.3 grams for neutralizing free fatty acids) in 2.4 litres of methanol, with a ratio of 200 ml methanol per litre of oil. NaOH was added gradually to ensure proper dissolution, forming sodium methoxide. The sodium methoxide solution was then added to the cotton seed oil and vigorously stirred to facilitate the reaction. During the process, the cloudy free fatty acids and glycerine separated and settled at the bottom of the reactor, while the fatty acid methyl ester (biodiesel), a clear translucent liquid, remained on the top. Stirring was stopped once the separation process began to plateau, and the mixture was allowed to settle overnight to ensure complete separation. The upper layer containing the fatty acid methyl ester (biodiesel) was carefully collected, but any remaining soaps or salts needed to be removed through further purification before use. The glycerine, which settled at the bottom, can be repurposed for applications such as cosmetic production. While the reactor was resting during the settling process, a new batch could be initiated to optimize the production efficiency.

The fatty acid methyl ester (biodiesel) was transferred into a clean container and thoroughly washed to remove any residual soaps and salts. Warm water was added to the methyl ester, and the mixture was gently swirled to allow separation. After settling, warm water was carefully drained from the bottom. This rinsing process was repeated until the discharged rinse water reached a neutral pH of 6−7 and was free of soap bubbles. The resulting liquid appeared hazy, indicating the presence of trapped water, which needed to be evaporated by gently heating the biodiesel. Any white solids settling at the bottom or bubbles forming on the surface were signs of residual soap; in such cases, further re-washing or removal was performed. Dehydration of the methyl ester was carried out at 100°C to ensure the final biodiesel product was free from moisture.

Blends of biodiesel with diesel fuel were prepared in varying proportions, analysed, and compared to pure diesel fuel. The blends included 15% flax methyl ester with 85% diesel, 10% flax methyl ester with 90% diesel, 5% flax methyl ester with 95% diesel, and 100% pure flax methyl ester.

To ensure uniform dispersion of nanoparticles in the biodiesel blend, a magnetic stirrer was initially used to mix the TiO_2 nanoparticles thoroughly with the biodiesel. This was followed by ultrasonication (ultrasonic agitation) to break up nanoparticle clusters, resulting in a stable and homogenous dispersion of TiO_2 within the blend. To minimize the risk of agglomeration during engine operation, fresh blends were prepared immediately before testing to reduce the chances of sedimentation. Additionally, the TiO_2 concentration was carefully optimized ($\leq$ 100 ppm), as higher concentrations are more prone to agglomeration. During engine operation, continuous fuel injection pressure and in-cylinder turbulence further aid in maintaining a uniform nanoparticle dispersion throughout the combustion process.

2.2. Estimation of thermophysical properties

Kinematic viscosity

The kinematic viscosity of several cotton seed biodiesel blends is evaluated using a Redwood viscometer as shown in Fig. 3a. This device does not provide a direct measurement of viscosity in absolute units, but it does allow for the comparison of oil viscosities by measuring the efflux of 50 ml of oil through the instrument's standard orifice under standard circumstances.

Fig. 3. Redwood viscometer set-up (a), Cleveland set-up (b), bomb calorimeter set-up (c).

Flash and fire point

The flash and fire points of each mix of biodiesel samples were evaluated as per IS1448 by using the Cleveland set-up. The oil sample under test was poured into an oil cup until it reached the mark. Figure 3b shows the equipment used to determine the flash and pour points. The gasoline sample was swirled at a modest continuous pace of around 60 rpm. The oil sample was heated at a rate of 5 to 6 degrees of Celsius per minute. A shudder was used to introduce flame for a brief period of time with each 1°C increase in temperature. The flash point was defined as the lowest temperature at which a clear flash was seen. The fire point was defined as the temperature at which fuel vapour ignites and remains in flames for at least five seconds.

Calorific value

The heat of combustion of fuel samples was evaluated using an IS1448-compliant Wilson Scientific Works isothermal bomb calorimeter, as illustrated in Fig. 3c. A 1ml fuel sample was burned in a calorimeter bomb with pure oxygen. The sample was ignited electrically. Temperature increase was measured as heat was generated. The water equivalent (effective heat capacity of the calorimeter) was also calculated using pure and dry benzoic acid as the test fuel. Every sample was repeated three times. The gross heat of combustion for the fuel samples was determined using the equation shown in Table 1.

Table 1. Kinematic viscosity of cotton seed biodiesel blends.

Kinematic viscosity	Calorific value
If $t_m < 34 \Rightarrow \nu = 0.24 \times t_m - 50/t_m$, If $t_m < 34 \Rightarrow \nu = 0.26 \times t_m - 179/t_m$,	$H_c = W_c \times \Delta T/M_s$,
where: t_m – mean time, s, ν – kinematic viscosity, cSt, H_c = heat combustion of the fuel sample, cal/g, W_c = water equivalent of the calorimeter, cal/°C, ΔT = rise in temperature, °C, M_s = mass of sample burnt, kg.	

The properties of various cottonseed biodiesel blends are presented in Table 2.

Table 2. Properties of different blends of cotton seed biodiesel.

Blends	Kinematic viscosity, cSt	Calorific value, kJ/kg	Flash point, °C	Fire point, °C	Density, g/cm³
Diesel	4.18	45270	60	64	0.81
Biodiesel	4.89	41760	172	184.4	0.874
B10	4.15	40890	71	77.2	0.82
B20	3.87	39640	82.4	89.6	0.81
B30	2.62	3710	91.7	97.5	0.79
B40	2.26	35110	103.8	110.2	0.792
B10+TiO_2	2.68	39750	77	83	0.841
B20+TiO_2	2.8	38170	87	93.5	0.849
B30+TiO_2	4.3	36190	96.4	101.9	0.857
B40+TiO_2	4.4	34260	106.2	112.3	0.861

3. Experimental set-up and procedure

The experimental setup consists of an engine, a dynamometer, and an exhaust gas analyser. The engine is a single cylinder, four stroke, vertical, water-cooled, direct injection computerised VCR CI engine, as shown in Fig. 4. The eddy current dynamometer comprises of a stator with electromagnets and a rotor disc that is connected to the engine's output shaft. When the rotor rotates, eddy currents form in the stator owing to the magnetic flux created by the passage of field current via the electromagnets. These eddy currents impede rotor rotation, therefore loading the engine.

These eddy currents enhance heat production. As a result, a cooling system is used to disperse the heat. A moment arm measures torque. The load is controlled by regulating the current using electromagnets. First, tighten the nut bolts on the engine, dynamometer, propeller shaft, and base frame. Ensure that the engine sump tank contains enough lubricating oil. This may be verified by marking the level stick. Ensure that there is enough fuel in the tank. Remove any air that may be in the fuel line. Turn on the electric power supply to the piezo powering unit (PPU)/AX-409, the dynamometer loading unit (DLU)/AX-155, the load indicator, and the voltmeter. Configure the engine model for configuration variables and system constants using the "Enginesoft" program on your computer. Start water circulation by using a water pump and adjust the flow rate of 250−350 l/h for the engine and 75−100 l/h for the calorimeter by regulating the valves provided at the rotameter inlet. Ensure that water is flowing through a dynamometer at a pressure of ~0.5−1 bar.

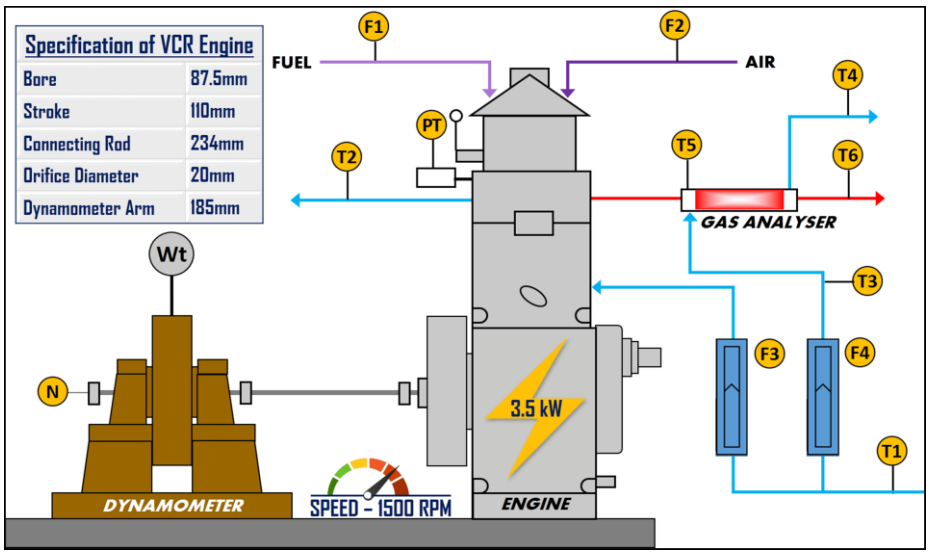

Fig. 4. Experimental set-up with instrumentation.

3.1. Factorial design of experimentation

Initially bypass the measuring tube as shown in Fig. 5 and allow the fuel to engine and adjust the knob on the dynamometer loading unit (DLU) for zero kg load and wait for 3 minutes to ensure the load is constant. To estimate the fuel consumption, regulate the valve to direct the fuel to the engine through the measuring tank. Measure the time for the consumption of 5cm^3 fuel under zero load. Again, bypass the measuring tube and change the load to 3 kg by using DLU. After ensuring the constant load reading, operate the valve to direct the fuel to the engine through the measuring tube. Measure the time for the consumption of 5 cm^3 fuel under 3 kg load. Repeat the above procedure for the different set of loads as shown in Table 3 and record data. After re-

cording all the required data, remove the load on the engine by using DLU, and Click "Scan Stop" on a PC. Stop the engine and allow the water to circulate for 5 minutes. All the blends and blends with TiO_2 have been tested, and data have been collected by repeating the above experimental procedure.

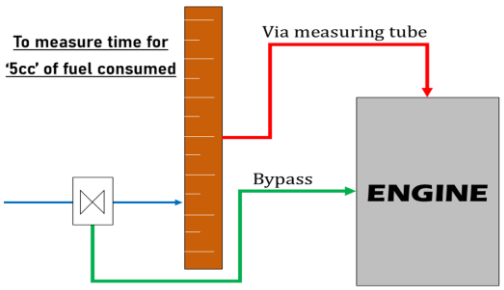

Fig. 5. Fuel flow configuration (to regulate the fuel flow direction) to conduct the experiments.

Table 3. Factorial design of experiments of diesel, B10, B20, B30, B40, B10+TiO_2, B10+TiO_2, B20+TiO_2, B30+TiO_2, B40+TiO_2.

Experiment number	Fuel flow direction	Regulate the DLU knob for load, kg	Record the time for fuel consumption, cm^3
1	Bypass measuring tube	0	5
	Through measuring tube	0	5
2	Bypass measuring tube	3	5
	Through measuring tube	3	5
3	Bypass measuring tube	6	5
	Through measuring tube	6	5
4	Bypass measuring tube	9	5
	Through measuring tube	9	5
5	Bypass measuring tube	12	5
	Through measuring tube	12	5

The exhaust emission parameters were determined using the AVL flue gas analyser. The AVL analyser was used to examine HC emissions. Furthermore, emission characteristics such as CO and nitrogen oxide (NO_x) were assessed. The sensors were installed into the exhaust gas outlet under each load state. The exhaust gases were fed through the analyser using sensors. At least three readings of the analyser digital screen were noted down, and the mean was be considered.

4. Results and discussion

The blends of varying proportions of flax methyl ester and diesel were prepared, analysed, and compared with diesel fuel. The different blends in the proportions of 10% alternative oil with 90% diesel, 20% alternative oil with 80% diesel, 30% alternative oil with 70% diesel, and 40% alternative oil with 60% diesel were tested in the present investigation. These blends were also tested by incorporating TiO_2 nanoparticles at a concentration of 30 ppm.

All the experiments were conducted under a 200 bar pressure with a compression ratio of 16:1. The experiments were conducted for the performance and emission characteristics of a cotton seed biodiesel prepared through the transesterification method, followed by volume-based blending with the addition of TiO_2. The parameters viz. brake thermal efficiency (η_{BTE}), mechanical efficiency (η_{ME}), fuel consumption (FC) and brake specific fuel consumption (BSFC) were estimated to examine the performance characteristics. Further, the fraction of CO, the fraction of HC, and the fraction of NO_x were estimated to examine the emission characteristics.

Figure 6 shows the variation of brake thermal efficiency (BTE) and the mechanical efficiency with respect to load. Figure 6a shows the increase in BTE for various cotton seed biodiesel blends, both with and without TiO_2, under different load conditions (3 kg, 6 kg, 9 kg, and 12 kg). The zero line denotes pure diesel, serving as a reference point. The biodiesel blends (B10, B20, B30, B40) show a noticeable increase in BTE compared to pure diesel under all loads. The biodiesel blends with TiO_2 exhibit higher BTE improvements than their corresponding biodiesel blends without TiO_2, suggesting that TiO_2 improves efficiency. The trend generally shows that higher biodiesel blends tend to yield greater efficiency improvements, with B40 + TiO_2

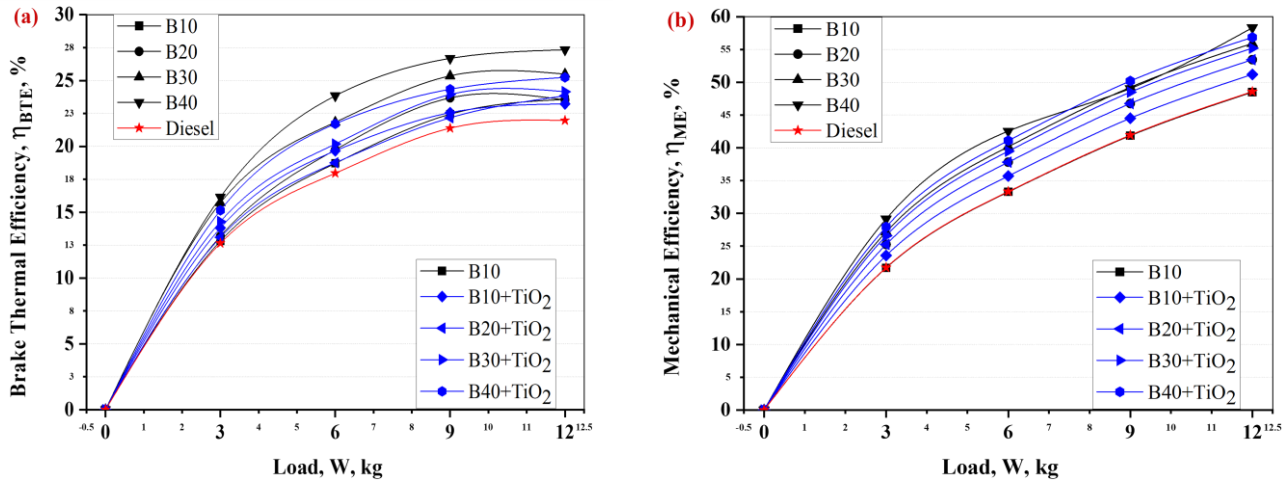

Fig. 6. Variation of efficiencies with load for different blend proportions (a) BTE (b) ME.

achieving the highest increase in BTE across most load conditions. The increase in BTE tends to be greater at higher loads for all fuel blends. The improved combustion behaviour with TiO_2 inclusion can be attributed to its catalytic properties, which promote surface oxidation reactions and enhance fuel-air mixing. Additionally, TiO_2 acts as an oxygen buffer, aiding in the oxidation of unburnt hydrocarbons and thereby improving overall combustion efficiency. However, the B40 blend without TiO_2 outperforms the TiO_2-enhanced blends in terms of brake thermal efficiency. This may be due to more complete combustion occurring at the higher pressures and temperatures present under full-load conditions, even without the aid of the catalyst.

The graph shown in Fig. 6b represents the variation of mechanical efficiency with respect to load for different fuel blends and diesel, with and without the addition of TiO_2 nanoparticles. The fuel blends containing TiO_2 exhibit reduced mechanical efficiency compared to their counterparts without TiO_2. However, this trade-off is considered worthwhile because the addition of TiO_2 helps reduce emissions. Diesel shows the lowest mechanical efficiency across all load values compared to the biodiesel blends, indicating that biodiesel blends (both with and without TiO_2) offer better efficiency. The blends B40 and B40 + TiO_2 show the highest mechanical efficiency values, especially at higher load levels. Figure 6b indicates that biodiesel blends, particularly those enhanced with TiO_2, can achieve better mechanical efficiency than conventional diesel fuel. However, the B40 blend without TiO_2 outperformed the TiO_2-enhanced blends in terms of mechanical efficiency. This can be attributed to the inherently higher oxygen content, better volatility, and improved atomization characteristics of the B40 blend, which facilitate more complete combustion. Although TiO_2 is known to promote oxidation, under full load conditions, its excessive thermal activity may lead to premature combustion, resulting in engine knocking and a subsequent reduction in mechanical efficiency.

Figure 7 depicts the relationship between fuel consumption and load for various fuel types, including biodiesel blends (B10, B20, B30, B40) and diesel, with and without the addition of TiO_2 nanoparticles. All fuel types exhibit the increased fuel consumption as the load on the engine increases, ranging from approximately 0.5 kg/h at zero load to over 1.2 kg/h at 12 kg load. The fuel blends with TiO2 show slightly higher fuel consumption compared to their non-TiO_2 counterparts at the cost of decrease of exhaust gas emissions with the addition of TiO_2 particles. The fuel consumption of cotton seed biodiesel blends has been decreased when compared with pure diesel by 1.3 % to 9.8%. While in the case of cotton seed biodiesel blends with addition of TiO_2 particles, the fuel consumption has been raised by 1.8% to 7.6% when compared to diesel.

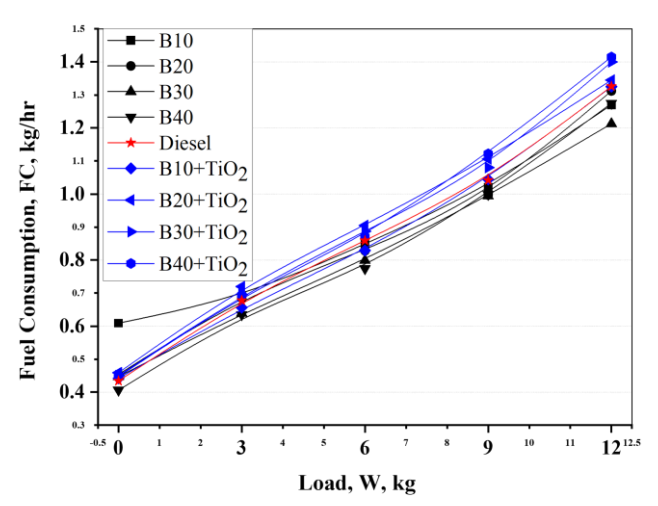

Fig. 7. Fuel consumption vs. load for different blend proportions.

Figure 8 depicts the fluctuation in brake specific fuel consumption (BSFC) with respect to the engine load with a compression ratio of 16:1. BSFC increases with all blends and diesel and gradually falls to full load for all blends and fuel. This is because when the load grows, the temperature within the cylinder rises, reducing the delay period. At full load, B10 has the lowest BSFC of any mix of diesel. At maximum load, the minimum BSFC for B10 is 0.373 kg/kWh.

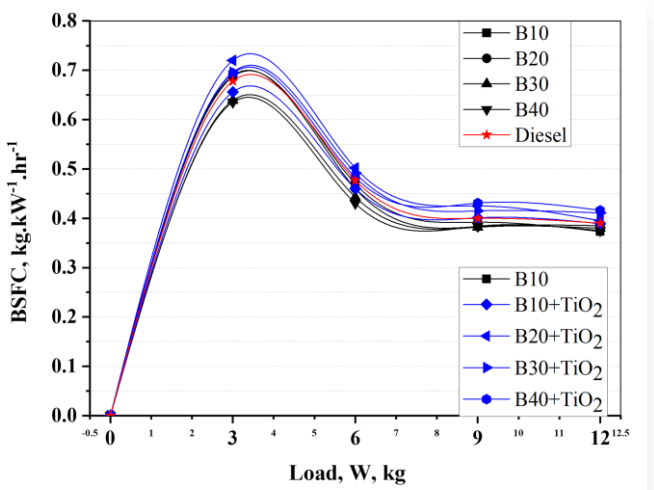

Fig. 8. BSFC vs. load for different blend proportions.

The graph shown in Fig. 8 illustrates the relationship between brake specific fuel consumption (BSFC) and load (kg) for different fuel blends, including biodiesel blends (B10, B20, B30, B40) and diesel, with and without the addition of titanium dioxide (TiO_2) nanoparticles. The addition of TiO_2 results in a slight improvement in fuel efficiency, as seen by the marginally lower BSFC values compared to their corresponding biodiesel blends without TiO_2. As the engine load increases from 3 kg to 12 kg, BSFC consistently decreases, suggesting that the engine operates more efficiently at higher loads. B10 shows the highest BSFC values among biodiesel blends, while higher biodiesel blends like B40 exhibit slightly lower BSFC values at the higher load ranges.

Figure 9a depicts the variation of HC emissions in parts per million (ppm) with respect to load (in kg) for various biodiesel blends and diesel, both with and without the addition of TiO_2 nanoparticles. The fuel blends are B10, B20, B30, and B40, while B10 + TiO_2, B20 + TiO_2, B30 + TiO_2, and B40 + TiO2 represent the respective blends with TiO_2. For all fuel types, HC emissions increase as the load increases, especially beyond 6 kg.

The trend is more pronounced in conventional diesel and biodiesel blends without TiO_2. Diesel exhibits the highest HC emissions across all load levels, with a sharp increase as load increases. Biodiesel blends without TiO_2 (B10, B20, B30, B40) show moderate HC emissions. Among these, B10 has the highest emissions, while B40 has the lowest. The addition of TiO2 nanoparticles significantly reduces HC emissions for all biodiesel blends (B10 + TiO_2, B20 + TiO_2, B30 + TiO_2, B40 + TiO_2) across the entire load range. B40 + TiO_2 shows the lowest HC emissions, highlighting the efficiency of the higher concentration biodiesel blend with TiO_2 in reducing emissions. B40 + TiO_2 achieves the minimum HC emissions at all load levels, indicating the effectiveness of using high biodiesel blends with TiO_2 nanoparticles for reducing HC emissions.

The graph shown in Fig. 9b shows the variation of CO emission (in ppm) with respect to load for various fuel types, including blends of biodiesel (B10, B20, B30, B40) and standard diesel. As the load increases, CO emissions also increase for all fuels, but the rate of increase varies across the fuels. The increase in CO emission becomes more pronounced at loads above 6 kg, with biodiesel blends generally producing higher emissions than pure diesel. Higher biodiesel content in the blend (e.g. B20, B40) appears to result in greater CO emissions as the load increases, suggesting a trade-off in CO emissions with biodiesel use. Diesel has the lowest CO emissions across all loads compared to biodiesel blends.

The graph shown in Fig. 9c represents the relationship between NO_x emissions (in ppm) and load (in kg) for various fuel types and biodiesel blends, including the effect of adding TiO_2 to the blends. B10 has the highest NO_x emissions as the load increases, reaching above 600 ppm at the highest load. B40 and B30 also exhibit high NO_x emissions as the load increases, but lower than B10, B10 + TiO_2 and other biodiesel blends with TiO_2 additives, which show reduced NO_x emissions compared to their non-additive counterparts, indicating the effectiveness of TiO_2 in reducing NO_x emissions. Adding TiO_2 to biodiesel blends appears to reduce NO_x emissions across all load conditions, with a significant drop observed when comparing the emissions of blends like B20, B30, and B40 with and without TiO_2.

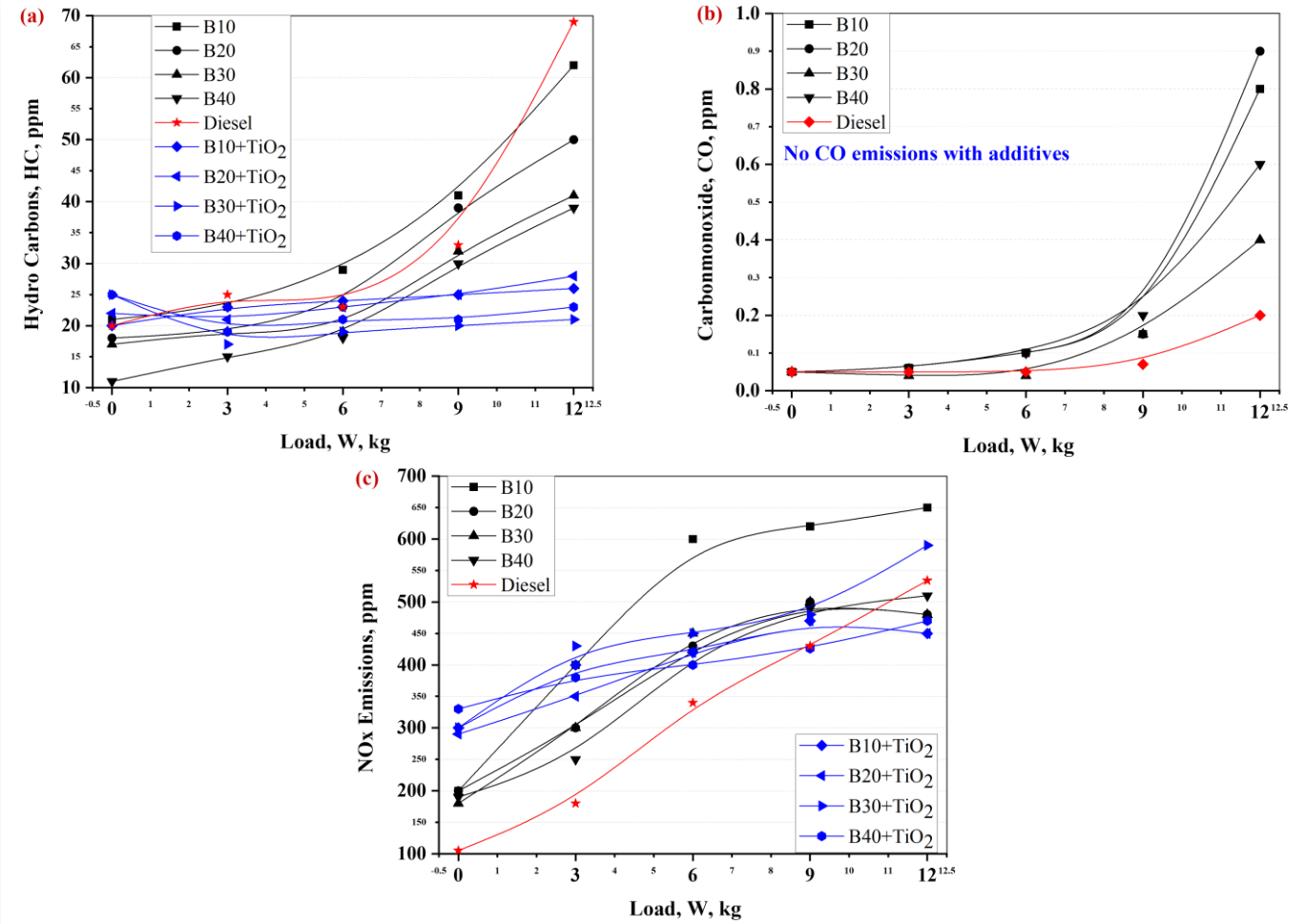

Fig. 9. Emission characteristics: (a) HC, (b) CO, (c) NO_x.

The increase of brake thermal efficiency (BTE) of different blends of cotton seed biodiesel with respect to diesel is quantified and shown in Fig. 10. In case of B10, the brake thermal efficiency has been increased by 1.3%, 4.1%, 4.9% and 7.2% for 3 kg, 6 kg, 9 kg and 12 kg loads, respectively. In the case of B20, the brake thermal efficiency has been increased by 16%, 13%, 11% and 10% for 3 kg, 6 kg, 9 kg and 12 kg loads, respectively. The fuel consumption has been decreased for B10, B20, B30 and B40, respectively. However, the fuel consumption is increased with the addition of TiO_2 particles.

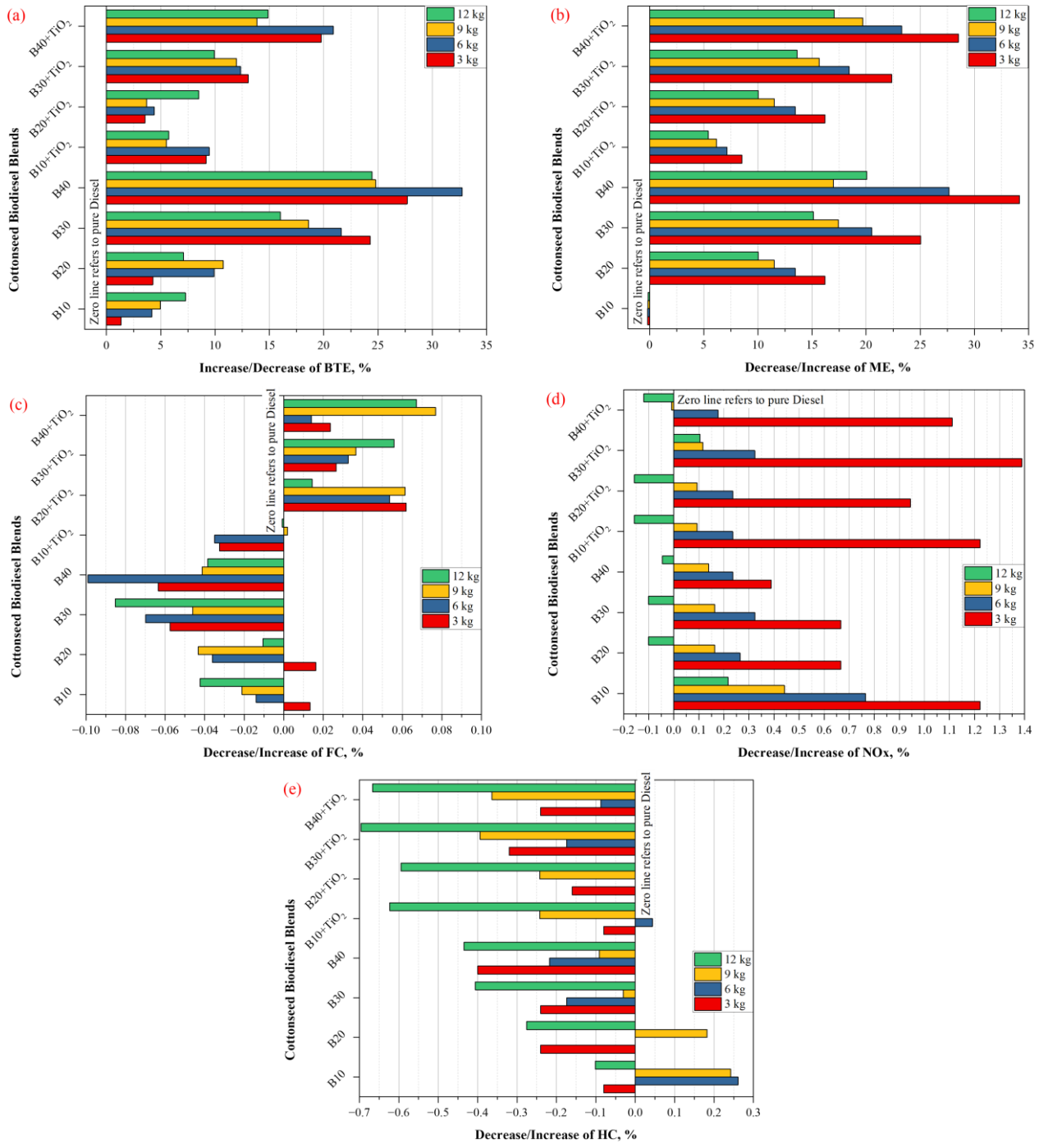

Fig. 10. Variation of performance and emission parameters of different blends of cotton seed biodiesel with respect to diesel: (a) BTE, (b) ME, (c) FC, (d) NO_x, (e) HC.

5. Conclusions

An experimental investigation was conducted to study the performance and emission characteristics of a variable compression ratio engine using various blend proportions, with and without additives, and compared to diesel. The key findings are as follows:

- Across all diesel blends, BTE improves as the temperature increases. Among the blends, B40 without additive achieved the highest BTE, surpassing diesel by 5.4%.
- Mechanical efficiency increases gradually with load for all blends. At full load, B40 without additive exhibited the highest mechanical efficiency at 58.31%, outperforming all other blends and diesel.
- Fuel consumption rises with engine load for all blends and diesel. B40 without additive demonstrated the lowest fuel economy at full load but still reduced fuel usage by 0.058 kg/h compared to diesel.
- Initially, BSFC increases for all blends and diesel, then decreases at full load. B10 without additive had the lowest

BSFC at full load, reducing BSFC by 0.017 kg/kWh compared to diesel.

- B10 without additive produced higher HC emissions than diesel up to 34% load but lower emissions at full load. The B40 blend without additive emitted fewer hydrocarbons than all other blends and diesel, reducing emissions by 34 ppm at full load, which corresponds to a 45% decrease compared to conventional diesel.
- CO emissions increased steadily from no load to full load for all blends without additives. The B30 blend without additive emitted less CO than diesel at half load. CO emissions were zero for all blends with additives, as TiO_2 promotes combustion, enhancing CO oxidation and reducing HC emissions.
- NO_x emissions increased with load for all blends and diesel. The addition of TiO_2 is beneficial in lowering NO_x emissions in biodiesel blends, especially for higher percentages of biodiesel content. NO_x emissions were reduced by 1.1% with the addition of TiO_2 in biodiesel blends (B40).

Beyond performance and emission improvements, the practical viability of TiO_2-enhanced biodiesel blends depends on factors such as cost, engine compatibility, and nanoparticle stability. Although TiO_2 is relatively low-cost and widely available, the long-term effects on engine wear, injector clogging, and catalyst degradation require further study. Moreover, ensuring uniform dispersion and preventing nanoparticle agglomeration during storage are essential for maintaining consistent combustion benefits. These considerations are vital for translating laboratory results into real-world applications.

Acknowledgements

We sincerely thank JNTU Kakinada for providing experimental support and IIT Roorkee for their valuable guidance in manuscript preparation. Their contributions have been helpful in the completion of this work.

References

[1] Bilal Ameer, H.M., Ameer, M.F., Ghachem, K., Ali, M., Razaq, A., Khan, S.U., Hamza, M., & Kolsi, L. (2022). Experimental comparison of performance and emission characteristics of 4-stroke CI engine operated with Roselle and Jatropha biodiesel blends. *Journal of the Indian Chemical Society*, 99(6), 100505. doi: 10.1016/j.jics.2022.100505

[2] Doğan, B., Yeşilyurt, M.K., Yaman, H., Korkmaz, N., & Arslan, A. (2024). Comprehensive analysis of a CI engine fuelled with blends of diesel fuel/safflower seed oil biodiesel/ TiO_2 or SiO_2 nanoparticles produced by green synthesis technique. *Process Safety and Environmental Protection*, 191, 417–438. doi: 10.1016/j.psep.2024.08.104

[3] Kailash, M.N., & Murali, G. (2024). Solar energy powered biodiesel synthesis from linseed oil – A novel experimental study. *Journal of the Indian Chemical Society*, 101, 101259. doi: 10.1016/j.jics.2024.101259

[4] Kanimozhi, B., Karthikeyan, L., Praveenkumar, T.R., Alharbi S.A., Alfarraj, S., & Gavurová, B. (2023). Evaluation of karanja and safflower biodiesel on engine's performance and emission characteristics along with nanoparticles in DI engine. *Fuel*, 352, 129101. doi: 10.1016/j.fuel.2023.129101

[5] Manap, M.R.A., Baharim, H.I., Shamsudin, N.A.A., & Ferdaus, A.F. (2024). Dataset of NIR, MIR and FIR spectroscopy of fuels in maritime cases and biodiesel–diesel blends B7 and B10 from Malaysia. *Data in Brief*, 55, 110615. doi: 10.1016/j.dib.2024.110615

[6] Adebisi, A., Abd-Rasheed, A., Olusegun, T., Sanni, S.E., Oguntade, T., & Oni B.A. (2023) . Effects of hydrogen enrichment on diesel engine fueled with Afzelia Africana biodiesel – TiO_2 blends. *Egyptian Journal of Petroleum*, 32(1), 81–86. doi: 10.1016/j.ejpe.2023.02.002

[7] Anjum, S.S., Prakash, O., Ahmad, S.N., & Pal, A. (2022). Optimization of biodiesel production from Argemone mexicana oil using Taguchi model. *Proceedings of the Institution of Mechanical Engineering, Part E: Journal of Process Mechanical Engineering*, 236(4), 1628–1636. doi: 10.1177/09544089221074839

[8] Dubba, S.K., & Kumar, R. (2017). Flow of refrigerants through capillary tubes: A state-of-the-art. *Experimental Thermal and Fluid Science*, 81, 370–381. doi: 10.1016/j.expthermflusci.2016.09.012

[9] Joshi, J.R., Bhanderi, K.K., & Patel, J.V. (2023). Waste cooking oil as a promising source for bio lubricants- A review. *Journal of the Indian Chemical Society*, 100, 100820. doi.: 10.1016/j.jics.2022.100820

[10] Nyorere, O., Oluka, S.I., Onoji, S.E., Nwadiolu, R., & Adepoju, T.F. (2024). Dataset on acido-biocatalysis of agro solid wastes in acidic medium for the conversion of pink solo *Carica papaya* seed oil to biodiesel fuel. *Data in Brief*, 53, 110219. doi: 10.1016/j.dib.2024.110219

[11] Nawaz, I.S.S., & Asokan, M.A. (2025). Numerical and experimental analysis on titanium aluminide and yttria stabilized zirconia coated piston on gulmohar biodiesel/diesel blend: An RSM approach. *Proceeding of the Institution of Mechanical Engineering, Part C: Journal of Mechanical Engineering Science*, 239(15). doi: 10.1177/09544062251333992

[12] Thangamani, J., Ismailgani, R., & Arunagirinathan, K. (2024). Toward sustainable transportation: Experimental insights into Chlorella vulgaris algae biodiesel with titanium oxide nano-enhancement. *Proceedings of the Institution of Mechanical Engineering, Part E: Journal of Process Mechanical Engineering*. doi: 10.1177/09544089241277707

[13] Singh, M., Saini, P., Divyanshi, S., Mishra, S., & Ahmad, S.N. (2025). Effect of n-pentanol with novel water hyacinth biodiesel-diesel ternary blends on diesel engine performance and emission characteristics. *Vietnam Journal of Chemistry*, 62(6), 780−791, Wiley Online Library. doi: 10.1002/vjch.202300383

[14] Alabi, O.O., Gbadeyan, O.J., Bala, A., Ogunsiji, G.O., & Deenadayalu, N. (2024). Study of combustion characteristics of diesel-vegetable oil blends utilizing an industrial fuel burner. *Fuel Communications*, 18, 100104. doi: 10.1016/j.jfueco.2023.100104

[15] Krupakaran, R.l., Hariprasasd, T., & Gopalakrishna, A. (2019). Experimental investigation on direct injection diesel engine fuelled with addition of titanium dioxide nanoparticle to M. elangi biodiesel for varying injection pressures. *Environmental Progress & Sustainable Energy*, 38(5), 13207. doi: 10.1002/ep.13207

[16] Jain, A., Bora, B.J., Kumar, R., Barik, D., Kumar, N., Paramasivam, P., Kumar, R., Chohan, J.S., Majdi, H.S., Alsubih, M., Islam, S., Prakash, C., & Kumar, R. (2025). Assessment of Nahar biodiesel with TiO_2 nanoparticles at increased fuel injection pressure of a diesel engine: Exergy, energy, statistical analysis. *Case Studies in Thermal Engineering*, 71, 106125. doi: 10.1016/j.csite.2025.106125

[17] Musthafa, M.M., Kumar, T.A., Mohanraj, T., & Chandramouli, R. (2018). A comparative study on performance, combustion and

emission characteristics of diesel engine fuelled by biodiesel blends with and without an additive. *Fuel*, 225, 343–348. doi: 10.1016/j.fuel.2018.03.147

[18] Shaik, J.H., Khayum, N., & Pandey, K.K. (2025). Analysis of combustion characteristics of a diesel engine run on ternary blends using machine learning algorithms. *Environmental Progress & Sustainable Energy*, 44(3), e14582. doi: 10.1002/ep.14582

[19] Radhakrishnan Lawrence, K., Tharigonda, H., & Alluru, G. (2020). An experimental investigations on combined effect of EGR and SCR for diesel engine fuelled with the addition of TiO_2 nanoparticle to M.Elangi methyl ester blend. *Australian Journal of Mechanical Engineering*, 18(2) 220–233. doi: 10.1080/14484846.2018.1519053

[20] Keskin, A., Yaşar, A., Yıldızhan, Ş., Uludamar, E., Emen, F.M., & Külcü, N. (2018). Evaluation of diesel fuel-biodiesel blends with palladium and acetylferrocene based additives in a diesel engine. *Fuel*, 216 349–355. doi: 0.1016/j.fuel.2017.11.154

[21] Jiaqiang, E., Zhang, Z., Chen, J., Pham, M., Zhao, X., Peng, Q., Zhang, B., & Yin, Z. (2018). Performance and emission evaluation of a marine diesel engine fueled by water biodiesel-diesel emulsion blends with a fuel additive of a cerium oxide nanoparticle. *Energy Conversion and Management*, 169, 194–205. doi: 10.1016/j.enconman.2018.05.073

[22] Mehregan, M., & Moghiman, M. (2018). Effects of nano-additives on pollutants emission and engine performance in a urea-SCR equipped diesel engine fueled with blended-biodiesel. *Fuel*, 222, 402–406. doi: 10.1016/j.fuel.2018.02.172

[23] Soudagar, M.E.M., Nik-Ghazali, N.-N., Kalam, M.A., Badruddin, I.A., Banapurmath, N.R., & Akram, N. (2018). The effect of nano-additives in diesel-biodiesel fuel blends: A comprehensive review on stability, engine performance and emission characteristics. *Energy Conversion and Management*, 178, 146–177. doi: 10.1016/j.enconman.2018.10.019